Research Article

Kamran*, Muhammad Asif, Aiman Mukheimer, Kamal Shah, Thabet Abdeljawad*, and Fahad M. Alotaibi

A comparative study of Bagley–Torvik equation under nonsingular kernel derivatives using Weeks method

https://doi.org/10.1515/phys-2023-0161
received August 17, 2023; accepted November 12, 2023

Abstract: Modeling several physical events leads to the Bagley–Torvik equation (BTE). In this study, we have taken into account the BTE, including the Caputo–Fabrizio and Atangana–Baleanu derivatives. It becomes challenging to find the analytical solution to these kinds of problems using standard methods in many circumstances. Therefore, to arrive at the required outcome, numerical techniques are used. The Laplace transform is a promising method that has been utilized in the literature to address a variety of issues that come up when modeling real-world data. For complicated functions, the Laplace transform approach can make the analytical inversion of the Laplace transform excessively laborious. As a result, numerical techniques are utilized to invert the Laplace transform. The numerical inverse Laplace transform is generally an ill-posed problem. Numerous numerical techniques for inverting the Laplace transform have been developed as a result of this challenge. In this article, we use the Weeks method, which is one of the most efficient numerical methods for inverting the Laplace transform. In our proposed methodology, first the BTE is transformed into an algebraic equation using Laplace transform. Then the reduced equation solved the Laplace domain. Finally, the Weeks method is used to convert the obtained solution from the Laplace domain into the real domain. Three test problems with Caputo–Fabrizio and Atangana–Baleanu derivatives are considered to demonstrate the accuracy, effectiveness, and feasibility of the proposed numerical method.

Keywords: Laplace transform, Bagley–Torvik equation, Caputo–Fabrizio derivative, Atangana–Baleanu derivative, numerical inversion, Weeks method, Laguerre polynomials

1 Introduction

A realistic modeling of a physical phenomenon, such as viscoelasticity, heat conduction, electrode–electrolyte polarization, electromagnetic waves, diffusion, and control theory, can be successfully accomplished by employing fractional calculus, which has caught the attention of a lot of investigators across many disciplines of applied science and engineering [1–4]. In this article, we consider the fractional Bagley–Torvik equation (BTE), first appeared in an innovative work [5]. Their work was about modeling the viscoelastic behavior of geological strata, metals, and glasses using fractional differential equations, demonstrating that this approach is successful in describing structures with both elastic and viscoelastic components. BTE is an extremely important equation used to solve many applied scientific and engineering problems. More specifically, BTE can be used to represent any linearly damped fractional oscillator with damping term having fractional derivative of order $\frac{3}{2}$. Particularly, the models of materials whose damping varies on frequency can be predicted by an equation with a $\frac{1}{2}$-order or $\frac{3}{2}$-order derivative. It may also model the motion of a rigid plate submerged in a viscous fluid and a

* **Corresponding author: Kamran,** Department of Mathematics, Islamia College Peshawar, Peshawar 25120, Khyber Pakhtunkhwa, Pakistan, e-mail: kamran.maths@icp.edu.pk
* **Corresponding author: Thabet Abdeljawad,** Department of Mathematics and Sciences, Prince Sultan University, Riyadh 11586, Saudi Arabia; Department of Medical Research, China Medical University, Taichung 40402, Taiwan; Department of Mathematics and Applied Mathematics, School of Science and Technology, Sefako Makgatho Health Sciences University, Ga-Rankuwa, South Africa, e-mail: tabdeljawad@psu.edu.sa
Muhammad Asif: Department of Mathematics, Islamia College Peshawar, Peshawar 25120, Khyber Pakhtunkhwa, Pakistan
Aiman Mukheimer: Department of Mathematics and Sciences, Prince Sultan University, Riyadh 11586, Saudi Arabia
Kamal Shah: Department of Mathematics and Sciences, Prince Sultan University, Riyadh 11586, Saudi Arabia; Department of Mathematics, University of Malakand, Chakdara, Dir(L), KPK, Pakistan
Fahad M. Alotaibi: Department of Information Systems, Faculty of Computing and Information Technology (FCIT), King Abdulaziz University, Jeddah 34025, Saudi Arabia

gas in a fluid, describing the motion of actual physical systems [2]. Generalized form of the BTE is written as follows:

$$a_1 D_\xi^\beta \mathcal{W}(\xi) + a_2 D_\xi^{\gamma+1} \mathcal{W}(\xi) + a_3 \mathcal{W}(\xi) = f(\xi), \quad 1 < \beta \le 2, \ 0 < \gamma \le 1, \tag{1}$$

with initial data

$$\mathcal{W}(0) = \mathcal{W}_0, \ \mathcal{W}'(0) = \mathcal{W}_1, \ \mathcal{W}_0, \mathcal{W}_1 \in \mathbb{R}.$$

We will consider Eq. (1) for $\beta = 2$ and $\gamma = \frac{1}{2}$. In literature, D_ξ^β and $D_\xi^{\gamma+1}$ fractional derivatives are used in Riemann–Liouville and Liouville–Caputo sense due to their convenient status. For example, Ji *et al.* [6] considered the BTE equation in Liouville–Caputo sense and studied its numerical solution using shifted Chebyshev operational matrix. Ray and Bera [7] obtained the solution of BTE using Adomian decomposition method. Jena and Chakraverty [8] obtained the analytic solution of BTE using Sumudu transformation. Çenesiz *et al.* [9] obtained the numerical solution of BTE using the generalized Taylor collocation method. Mashayekhi and Razzaghi [10] studied the numerical solution of BTE using the hybrid functions approximation. They also derived the error bounds for the presented method. Gülsu *et al.* [11] utilized the Taylor matrix method for the approximation of the solution of BTE. In the study by Yüzbaşı [12], the numerical solution of BTE was obtained *via* the Bessel collocation method. In the study by Pinar [13], the authors obtained the analytic solution of BTE with conformable fractional derivative using the sine-Gordon expansion method and the Bernouli equation method. Raja *et al.* [14] studied the solution of BTE system arising in fluid dynamic model *via* feed-forward fractional artificial neural networks and sequential quadratic programming algorithm. However, these derivatives contain singular kernels, and they face problems when trying to model nonlocal phenomenon.

Caputo and Fabrizio in 2015 introduced a new fractional differential operator based on the exponential kernel function known as Caputo–Fabrizio derivative (CFD) to overcome the problem of the singular kernel function involved in the Riemann–Liouville and Liouville–Caputo fractional differential operators [16]. They demonstrated that CFD was suitable for modeling some physical problems. Atangana and Alqahtani [17] used the CFD for modeling the ground water pollution. Hasan *et al.* [18] studied the numerical solution of BTE under the CFD using a modified reproducing kernel Hilbert space method. Al-Smadi *et al.* [19] studied the solution of a nonlinear differential equation with CFD using a reproducing kernel algorithm. Moore *et al.* [20] developed a CFD model for HIV/AIDS epidemic. They obtained the numerical solution of the proposed model using a three step Adams–Bashforth predictor method. Joshi *et al.* [21] framed a fractional order mathematical model in the sense of CFD, to investigate the role of buffer and calcium concentration on fibroblast cells. For more information on CFD the readers can refer to the previous studies [22–24]. However, some issues were also pointed out against the considered derivatives, as the kernel in integral was nonsingular but was not nonlocal.

To overcome these issues, Atangana and Baleanu [25] proposed a new fractional operator based upon the Mittag–Leffler function known as Atangana–Baleanu derivative (ABD). Their operator includes a nonlocal and nonsingular kernel with all the benefits of Riemann–Liouville, Liouville–Caputo, and Caputo–Fabrizio operators. In addition to these features, the derivative was found very useful in thermal science material. Due to these powerful features, researchers have applied it to many phenomena [26,27]. Atangana [28] applied the ABD to the nonlinear Fisher's reaction–diffusion equation and obtained the solution of the modified equation using an iterative scheme. Gómez-Aguilar *et al.* [29] applied the ABD to electromagnetic waves in dielectric media. Ghanbari *et al.* [30] applied the ABD to three species predator-prey model. They obtained the desired solution using the product integration rule. Khan *et al.* [31] studied some necessary and sufficient conditions for the existence of the solutions of differential equations with modified ABD. Joshi *et al.* [32] proposed a nonsingular SIR model with the Mittag–Leffler law. The author used the nonlinear Beddington–DeAngelis infection rate and Holling type II treatment rate. The qualitative properties of the SIR model and the local and global stability of the model were also discussed. More information on the applications of ABD can be found in previous studies [33–38].

The goal of this study is to use both the Caputo–Fabrizio and ABDs with fractional order to extend the BTE to the realm of fractional calculus. In this work, we have used the Laplace transform method for this purpose. However, using the Laplace transform some times makes the analytic inversion very hard to compute for complicated functions. The literature on the numerical inversion of Laplace transform is extensive. Readers looking for a survey on the comparison of numerical inverse Laplace transform methods should begin with [39] and then proceed to the more recent work [40]. The numerical comparisons reported in these articles reveal supremacy of three numerical methods: the Talbot's method, the enhanced trapezoidal rule, and the Weeks method. The latter method is the subject of the current study, specifically the issue of choosing the two free parameters that determine method's accuracy. The Weeks method holds one major advantage over the Talbot's method and the enhanced trapezoidal rule: In particular, it assumes that a smooth function can be well approximated by an expansion in terms of

orthonormal Laguerre functions [41]. Laguerre functions are used because the quadrature formulas involving them are similar to the Laplace transform operator. In this method, the unknown coefficients are evaluated once for all for any given transformed function. It is highly efficient for multiple evaluations in the time domain. Computing the function at a new time with these other methods requires essentially restarting the numerical inversion procedure. Furthermore, it is equally applicable to real and complex time-domain functions [42].

2 Basic definitions

Here, we present some important definitions related to our work.

Definition 2.1. The Caputo derivative of a function $\mathcal{W}(\xi)$ with fractional order $\gamma \in (l-1, l]$, $l \in \mathbb{Z}^+$ is defined as follows [1]:

$$ {}_{\eta}^{C}D_{\xi}^{\gamma}\mathcal{W}(\xi) = \frac{1}{\Gamma(l-\gamma)}\int_0^{\xi}\frac{\frac{\mathrm{d}^l\mathcal{W}(s)}{\mathrm{d}s^l}}{(\xi-s)^{\gamma-l+1}}\mathrm{d}s. \tag{2}$$

Definition 2.2. Let $\mathcal{W} \in \mathcal{H}^l(\eta, \delta)$, $\delta > \eta$,$\gamma \in (l-1, l]$, $l \in \mathbb{Z}^+$ and not necessarily differentiable, then the CFD with base point η at point $\xi \in (\eta, \delta)$ is defined as follows [25]:

$$ {}^{\mathrm{CFD}}_{\eta}D_{\xi}^{\gamma}\mathcal{W}(\xi) = \frac{\mathcal{G}(\gamma)}{1-\gamma}\int_{\eta}^{\xi}\frac{\mathrm{d}^l\mathcal{W}(s)}{\mathrm{d}s^l}e^{\left[\frac{-\gamma}{1-\gamma}(\xi-s)\right]}\mathrm{d}s, \tag{3}$$

where $\mathcal{G}(\gamma) = 1-\gamma+\frac{\gamma}{\Gamma(\gamma)}$.

Definition 2.3. Let $\mathcal{W} \in \mathcal{H}^l(\eta, \delta)$, $\delta > \eta$,$\gamma \in (l-1, l]$, $l \in \mathbb{Z}^+$, then the ABD with base point η at point $\xi(\eta, \delta)$ is defined as follows [25]:

$$ {}^{ABD}_{\eta}D_{\xi}^{\gamma}\mathcal{W}(\xi) = \frac{\mathcal{G}(\gamma)}{1-\gamma}\int_{\eta}^{\xi}\frac{\mathrm{d}^l\mathcal{W}(s)}{\mathrm{d}s^l}E_{\gamma}\left[\frac{-\gamma}{1-\gamma}(\xi-s)^{\gamma}\right]\mathrm{d}s, \tag{4}$$

where $E_{\gamma}(\xi) = \sum_{k=0}^{\infty}\frac{\xi^k}{\Gamma(\gamma k+1)}$ is Mittag–Leffler function and $\mathcal{H}^l$ is the lth-order Sobolev space on a domain $\Omega \subset \mathbb{R}$ defined as $\mathcal{H}^l(\Omega) = \{\mathcal{W} \in L^2(\Omega) : \mathcal{W}^m \in L^2(\Omega),\ \forall m \le l\}$.

Definition 2.4. The Laplace transform of a piecewise continuous function $\mathcal{W}(\xi)$ for $\xi > 0$ is defined as follows [2]:

$$ \mathcal{L}\{\mathcal{W}(\xi)\} = \widehat{\mathcal{W}}(z) = \int_0^{\infty}e^{(-z\xi)}\mathcal{W}(\xi)\mathrm{d}\xi, \tag{5}$$

where z is the Laplace parameter.

Definition 2.5. If $l \in \mathbb{N}$, $\gamma \in [0, 1]$, then the Laplace transform of the CFD of a function $\mathcal{W}(\xi)$ is defined as follows [25]:

$$ \begin{aligned}\mathcal{L}\{{}^{\mathrm{CFD}}_{0}D_{\xi}^{\gamma+l}\mathcal{W}(\xi)\} = \frac{1}{z+\gamma(1-z)}[&z^{l+1}\widehat{\mathcal{W}}(z) - z^l\mathcal{W}(0)\\ &- z^{l-1}\mathcal{W}'(0) - \cdots - \mathcal{W}^l(0)],\end{aligned} \tag{6}$$

if $l = 0$, then

$$ \mathcal{L}\{{}^{\mathrm{CFD}}_{0}D_{\xi}^{\gamma}\mathcal{W}(\xi)\} = \frac{1}{z+\gamma(1-z)}[z\widehat{\mathcal{W}}(z) - \mathcal{W}(0)], \tag{7}$$

and if $l = 1$, then we have

$$ \begin{aligned}\mathcal{L}\{{}^{\mathrm{CFD}}_{0}D_{\xi}^{\gamma+1}\mathcal{W}(\xi)\} = \frac{1}{z+\gamma(1-z)}[&z^2\widehat{\mathcal{W}}(z) - z\mathcal{W}(0)\\ &- \mathcal{W}'(0)].\end{aligned} \tag{8}$$

Definition 2.6. The Laplace transform of ABD of a function $\mathcal{W}(\xi)$ is defined as follows [25]:

$$ \mathcal{L}\{{}^{\mathrm{ABD}}_{0}D_{\xi}^{\gamma}\mathcal{W}(\xi)\} = \frac{Q(\gamma)}{z^{\gamma}(1-\gamma)+\gamma}[z^{\gamma}\widehat{\mathcal{W}}(z) - z^{\gamma-1}\mathcal{W}(0)]. \tag{9}$$

3 Proposed scheme

This section covers the proposed numerical scheme for modeling BTE with CFD and ABD. The method has three major steps: (i) first, a BTE with CFD/ABD is considered and transformed to an algebraic equation *via* the Laplace transform; (ii) second, the reduced equation is solved in Laplace transform domain; (iii) finally, the desired solution is retrieved using numerical inverse Laplace transform method.

3.1 BTE with CFD

We consider BTE with CFD as follows:

$$ \begin{aligned}&a_1D_{\xi}^{\beta}\mathcal{W}(\xi) + a_2{}^{\mathrm{CFD}}_{0}D_{\xi}^{\gamma+1}\mathcal{W}(\xi) + a_3\mathcal{W}(\xi) = f(\xi),\\ &l-1 < \gamma \le l,\end{aligned} \tag{10}$$

with initial conditions

$$ \mathcal{W}^{(j)}(0) = \mathcal{W}_0^{(j)}, \quad j = 0, 1, \ldots, l-1. \tag{11}$$

By taking the Laplace transform of Eq. (10), we obtain

$$ \begin{aligned}&\mathcal{L}\{a_1D_{\xi}^{\beta}\mathcal{W}(\xi) + a_2{}^{\mathrm{CFD}}_{0}D_{\xi}^{\gamma+1}\mathcal{W}(\xi) + a_3\mathcal{W}(\xi)\}\\ &= \mathcal{L}\{f(\xi)\},\end{aligned} \tag{12}$$

which implies

$$a_1[z^\beta\widehat{\mathcal{W}}(z) - z^{\beta-1}\mathcal{W}(0) - z^{\beta-2}\mathcal{W}'(0)] + a_2\left[\frac{1}{z+\gamma(1-z)}[z^2\widehat{\mathcal{W}}(z) - z\mathcal{W}(0) - \mathcal{W}'(0)]\right] + a_3\widehat{\mathcal{W}}(z) = \hat{F}(z). \tag{13}$$

By solving for $\widehat{\mathcal{W}}(z)$, we obtain

$$\widehat{\mathcal{W}}(z) = \frac{a_1z^{\beta-1}\mathcal{W}(0) + a_1^{\beta-2}\mathcal{W}'(0) + \frac{a_2z\mathcal{W}(0)}{z+\gamma(1-z)} + \frac{a_2\mathcal{W}'(0)}{z+\gamma(1-z)} + \hat{F}(z)}{a_1z^\beta + \frac{a_2z^2}{z+\gamma(1-z)} + a_3}. \tag{14}$$

3.2 BTE with ABD

We consider BTE with ABD as follows:

$$a_1D_\xi^\beta\mathcal{W}(\xi) + a_2{}^{ABD}_0D_\xi^{\gamma+1}\mathcal{W}(\xi) + a_3\mathcal{W}(\xi) = f(\xi). \quad l-1 < \gamma \le l, \tag{15}$$

with initial conditions

$$\mathcal{W}^{(j)}(0) = \mathcal{W}_0^{(j)}, \quad j = 0, 1, \ldots, p-1. \tag{16}$$

By taking the Laplace transform of Eq. (15), we obtain

$$\mathcal{L}\{a_1D_\xi^\beta\mathcal{W}(\xi) + a_2{}^{ABD}_0D_\xi^{\gamma+1}\mathcal{W}(\xi) + a_3\mathcal{W}(\xi)\} = \mathcal{L}\{f(\xi)\}, \tag{17}$$

which implies

$$a_1[z^\beta\widehat{\mathcal{W}}(z) - z^{\beta-1}\mathcal{W}(0) - z^{\beta-2}\mathcal{W}'(0)] + a_2\left[\frac{\mathcal{G}(\gamma+1)}{(1-z^{\gamma+1})\gamma+1}[z^{\gamma+1}\widehat{\mathcal{W}}(z) - z^\gamma\mathcal{W}(0) - z^{\gamma-1}\mathcal{W}'(0)]\right] + a_3\widehat{\mathcal{W}}(z) = \hat{F}(z). \tag{18}$$

Solving for $\widehat{\mathcal{W}}(z)$, we obtain

$$\widehat{\mathcal{W}}(z) = \frac{a_1z^{\beta-1}\mathcal{W}(0) + a_1z^{\beta-2}\mathcal{W}'(0) + \frac{a_2\mathcal{G}(\gamma+1)z^\gamma\mathcal{W}(0)}{(1-z^{\gamma+1})\gamma+1} + \frac{a_2\mathcal{G}(\gamma+1)z^{\gamma-1}\mathcal{W}'(0)}{(1-z^{\gamma+1})\gamma+1} + \hat{F}(z)}{a_1z^\beta + \frac{a_2\mathcal{G}(\gamma+1)z^{\gamma+1}}{(1-z^{\gamma+1})\gamma+1} + a_3}. \tag{19}$$

3.3 Inverse Laplace transform

By taking the inverse Laplace transform of (14) or (19), we have

$$\mathcal{W}(\xi) = \frac{1}{2\pi i}\int_{\sigma-i\infty}^{\sigma+i\infty}\widehat{\mathcal{W}}(z)e^{z\xi}\mathrm{d}z = \frac{1}{2\pi i}\int_\Theta\widehat{\mathcal{W}}(z)e^{z\xi}\mathrm{d}z, \ \sigma > \sigma_0. \tag{20}$$

The integral in Eq. (20) is known as Bromwich integral, σ_0 is the abscissa of convergence, and Θ is an appropriately selected line joining $\sigma - i\infty$ and $\sigma + i\infty$ to restrict all the singularities of the transform function $\widehat{\mathcal{W}}(z)$ to the left of Θ. The analytic computation of the integral in Eq. (20) can be hard for complicated functions. Therefore, the research community have developed various approaches for the numerical approximation of the integral in Eq. (20). Each individual approach has its own application and is suitable for a specific problem. All the approaches are based on approximations used to evaluate the integral given in Eq. (20). In the current study, we use the Weeks method for the numerical approximation of the integral in Eq. (20).

3.4 Weeks method

The Weeks method is one of the most effective numerical strategies for inverting the Laplace transform, as long as the two free parameters in the Laguerre expansion on which it is based are chosen well. The Weeks technique has one significant benefit over the enhanced trapezoidal rule and Talbot's method: it gives a function expansion, notably the Laguerre series expansion. This indicates that for each given $\widehat{\mathcal{W}}(z)$, the unknown coefficients in the Laguerre series expansion may be determined once and for all. In Weeks method, the Bromwich line is parameterized as $z = \sigma + iy, y \in \mathbb{R}$ to obtain the Fourier integral

$$\mathcal{W}(\xi) = \frac{e^{\sigma\xi}}{2\pi}\int_{-\infty}^{\infty}e^{i\xi y}\widehat{\mathcal{W}}(\sigma+iy)\mathrm{d}y. \tag{21}$$

The function $\widehat{\mathcal{W}}(\sigma + iy)$ is expanded as follows:

$$\widehat{\mathcal{W}}(\sigma + iy) = \sum_{k=-\infty}^{\infty} a_k \frac{(-\varsigma + iy)^k}{(\varsigma + iy)^{k+1}}, \ \varsigma > 0, \ y \in \mathbb{R}. \quad (22)$$

By using Eq. (22) in Eq. (21), we obtain

$$\mathcal{W}(\xi) = \frac{e^{\sigma\xi}}{2\pi} \sum_{k=-\infty}^{\infty} a_k \psi_k(\xi; \varsigma), \quad (23)$$

where

$$\psi_k(\xi; \varsigma) = \int_{-\infty}^{\infty} e^{i\xi y} \frac{(-\varsigma + iy)^k}{(\varsigma + iy)^{k+1}} \mathrm{d}y. \quad (24)$$

We may use residues to evaluate the Fourier integral, and for $\xi > 0$, one obtains

$$\psi_k(\xi; \varsigma) = \begin{cases} 2\pi e^{-\varsigma\xi} L_k(2\varsigma\xi), & k \geq 0, \\ 0, & k < 0, \end{cases} \quad (25)$$

where $L_k(\xi)$ is Laguerre polynomial of degree k, $\sigma > \sigma_0$, σ_0 is the abscissa of convergence, and $\sigma, \varsigma \in \mathbb{R}$ are positive parameters. The polynomials $L_k(\xi)$ are defined as follows:

$$L_k(\xi) = \frac{e^{\xi}}{k!} \frac{\mathrm{d}^k}{\mathrm{d}\xi^k}(e^{-\xi}\xi^k), \quad (26)$$

where a_k denotes the coefficients in the Taylor series. See (Figure 1):

$$Q(\omega) = \frac{2\varsigma}{1-\omega} \widehat{\mathcal{W}}\left(\sigma + \frac{2\varsigma}{1-\omega} - \varsigma\right) = \sum_{k=0}^{\infty} a_k \omega^k, \ |\omega| < R, \quad (27)$$

where R denotes the radius of convergence of the Maclaurin series (27). The coefficients a_k are computed as follows:

$$a_k = \frac{1}{2\pi i} \int_{|\omega|=1} \frac{Q(\omega)}{\omega^{k+1}} \mathrm{d}\omega = \frac{1}{2\pi} \int_{-\pi}^{\pi} Q(e^{i\vartheta}) e^{-ik\vartheta} \mathrm{d}\vartheta. \quad (28)$$

The integral in Eq. (28) is the well-known Cauchy's formula, which can be approximated as follows:

$$\tilde{a}_k = \frac{e^{-ikh/2}}{2M} \sum_{j=-M}^{M-1} Q(e^{i\vartheta_{j+1/2}}) e^{-ik\vartheta_j}, \ k = 0, 1, 2, \ldots, M-1, \quad (29)$$

where $\vartheta_j = jh$, $h = \frac{\pi}{M}$.

3.4.1 Error analysis of the method

This section is devoted to the error analysis. Weideman [43] analyzed the error of the Weeks method. The following observations were made during their study for the following expansion:

$$\mathcal{W}(\xi) = \exp(\sigma\xi) \sum_{k=0}^{\infty} a_k \exp(-\varsigma\xi) L_k(2\varsigma\xi). \quad (30)$$

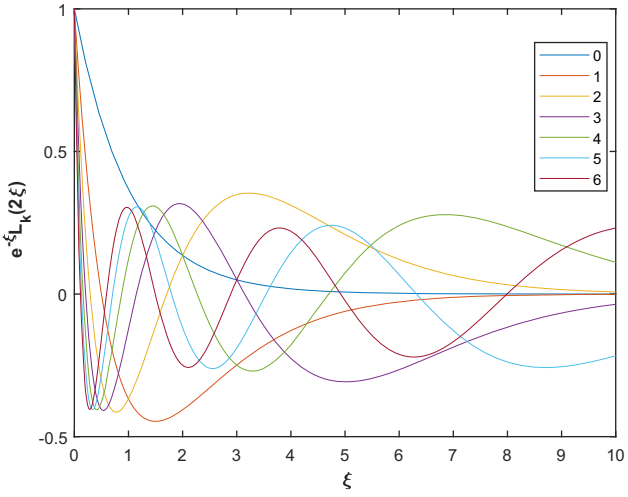

Figure 1: Laguerre polynomials of orders 0 through k.

Three main factors that contribute to error were identified:

- The first factor is truncating the series at M terms.
- The numerical computation of the coefficients is the second factor.
- Third is the inversion of Laplace transform numerically. Any inaccuracy in the evaluated coefficients increases with rising ξ when $\sigma > 0$, which is how the error in (30) may be seen.

To model these three factors of error, the real expansion is

$$\tilde{\mathcal{W}}(\xi) = \exp(\sigma\xi) \sum_{k=0}^{N-1} \tilde{a}_k (1 + \varpi_k) \exp(-\varsigma\xi) L_k(2\varsigma\xi), \quad (31)$$

where ϖ_k denotes the relative error of the coefficients in the floating-point representation, *i.e.*, $fl(\tilde{a}_k) = \tilde{a}_k(1 + \varpi_k)$. From Eqs (31) and (30), we have

$$|\mathcal{W}(\xi) - \tilde{\mathcal{W}}(\xi)| \leq \exp(\sigma\xi)(T(\text{error}) + D(\text{error}) + C(\text{error})),$$

with assumption $\sum_{k=0}^{\infty} |a_k| < \infty$, where $T(\text{error}) = \sum_{k=M}^{\infty} |a_k|$ is the truncation error bound, $D(\text{error}) = \sum_{k=0}^{M-1} |a_k - \tilde{a}_k|$ is the discretization error bound , $C(\text{error}) = \varpi \sum_{k=0}^{M-1} |\tilde{a}_k|$ is the conditioning error bound, and ϖ_k denotes the roundoff unit of machine satisfying the condition $\max_{0 \leq k \leq M-1} |\varpi_k| \leq \varpi$ with the fact that $|\exp(-\varsigma\xi) L_k(2\varsigma\xi)| \leq 1$. We can neglect the $D(\text{error})$ in comparison with $T(\text{error})$ and $C(\text{error})$ [43]. Therefore, we refer to $T(\text{error})$ and $C(\text{error})$. For $T(\text{error})$ and $C(\text{error})$, the upper bound were reported as follows [43]:

$$T(\text{error}) \leq \frac{k(\chi)}{\chi^M(\chi - 1)}, \ C(\text{error}) \leq \varpi \frac{\chi k(\chi)}{\chi - 1},$$

which holds for $\chi \in (1, R)$. Therefore, we have the following error bound:

Table 1: The AbS(error), RlE(error), and $\text{error}_{\text{est}}$ corresponding to Problem 1

M	σ		ς		AbS(error)		RlE(error)		$\text{error}_{\text{est}}$	
	ABD	CFD	ABD	CFD	ABD	CFD	ABD	CFD	ABD	CFD
0.1	2.6146	3.4347	1.8936	1.2117	1.7347×10^{-18}	1.7347×10^{-18}	1.1565×10^{-16}	1.1565×10^{-16}	4.8094×10^{-16}	1.5691×10^{-16}
0.2	3.3654	3.4708	1.1703	1.1481	6.9389×10^{-18}	6.9389×10^{-18}	1.1565×10^{-16}	1.1565×10^{-16}	2.2407×10^{-16}	2.1615×10^{-16}
0.3	2.6146	3.1652	1.8936	1.1481	2.7756×10^{-17}	2.7756×10^{-17}	2.0560×10^{-16}	2.0560×10^{-16}	8.1133×10^{-16}	3.2886×10^{-16}
0.4	2.6146	3.1652	1.8936	1.1481	5.5511×10^{-17}	2.7756×10^{-17}	2.3130×10^{-16}	1.1565×10^{-16}	1.0538×10^{-15}	4.5131×10^{-16}
0.5	2.7000	3.4708	3.3401	1.4116	1.1102×10^{-16}	5.5511×10^{-17}	2.9606×10^{-16}	1.4803×10^{-16}	1.5692×10^{-15}	6.2770×10^{-16}
0.6	2.7000	3.4511	3.3401	1.3399	1.1102×10^{-16}	1.1102×10^{-16}	2.0560×10^{-16}	2.0560×10^{-16}	2.0556×10^{-15}	8.1381×10^{-16}
0.7	2.7000	3.1472	3.3401	1.1703	1.1102×10^{-16}	1.1102×10^{-16}	1.5105×10^{-16}	1.5105×10^{-16}	2.6928×10^{-15}	1.1399×10^{-15}
0.8	2.7000	3.1472	3.3401	1.1703	3.3307×10^{-16}	3.3307×10^{-16}	3.4694×10^{-16}	3.4694×10^{-16}	3.5275×10^{-15}	1.5615×10^{-15}
0.9	2.7000	3.1472	3.3401	1.1703	2.2204×10^{-16}	2.2204×10^{-16}	1.8275×10^{-16}	1.8275×10^{-16}	4.6209×10^{-15}	2.1391×10^{-15}
1	3.2934	2.5881	1.1703	0.8872	2.2204×10^{-16}	2.2204×10^{-16}	1.4803×10^{-16}	1.4803×10^{-16}	3.2704×10^{-15}	2.2446×10^{-15}

$$\text{error}_{\text{est}} \leq \frac{k(\chi)}{\chi^{M}(\chi - 1)} + \varpi \frac{\chi k(\chi)}{\chi - 1}. \tag{32}$$

To have an optimal value of $\text{error}_{\text{est}}$, Weideman [43] proposed two algorithms for obtaining the optimal values of σ and ς. We have used Algorithm 1:

Algorithm 1: Algorithm for optimal values of (σ, ς)

The algorithm requires $\mathcal{W}(z)$, ξ, and M, and $[\sigma_0, \sigma_{\max}] \times [0, \varsigma_{\max}]$ which are expected to have the best values of σ and ς. The algorithm then operates as follows:

$$\sigma = \{\sigma \in [\sigma_0, \sigma_{\max}] | \text{error}_{\text{est}}(\sigma, \varsigma(\sigma)) = \text{minimum}\},$$

where

$$\varsigma(\sigma) = \{\varsigma \in [0, \varsigma_{\max}] | T(\text{error})(\sigma, \varsigma) = \text{minimum}\}.$$

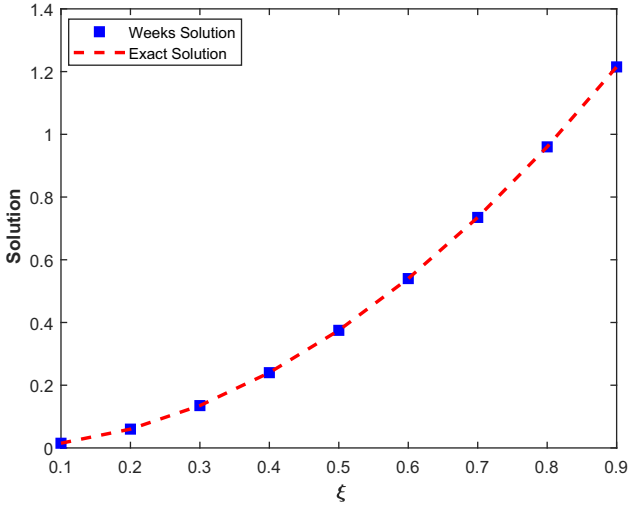

Figure 2: Exact solution *vs* Weeks solution of problem 1.

Table 2: The AbS(error), RlE(error), and $\text{error}_{\text{est}}$ corresponding to Problem 1

M	σ		ς		AbS(error)		RlE(error)		$\text{error}_{\text{est}}$	
	ABD	CFD	ABD	CFD	ABD	CFD	ABD	CFD	ABD	CFD
40	4.9699	4.2745	3.1153	2.4922	4.4409×10^{-16}	2.2204×10^{-16}	2.9606×10^{-16}	1.4803×10^{-16}	6.2431×10^{-15}	5.7162×10^{-15}
45	4.3000	2.5069	2.0592	1.8034	2.2204×10^{-16}	0	1.4803×10^{-16}	0	5.0408×10^{-15}	2.4480×10^{-15}
50	3.8254	2.4621	1.7308	1.1146	4.4409×10^{-16}	2.2204×10^{-16}	2.9606×10^{-16}	1.4803×10^{-16}	3.5918×10^{-15}	2.1400×10^{-15}
55	3.1754	2.5209	1.6716	1.1930	2.2204×10^{-16}	0	1.4803×10^{-16}	0	3.1507×10^{-15}	2.5050×10^{-15}
60	3.2776	3.3708	1.4373	1.2837	2.2204×10^{-16}	2.2204×10^{-16}	1.4803×10^{-16}	2.9606×10^{-16}	3.2848×10^{-15}	3.1068×10^{-15}
65	3.1652	2.4074	1.0677	0.8610	2.2204×10^{-16}	2.2204×10^{-16}	1.4803×10^{-16}	1.4803×10^{-16}	2.9024×10^{-15}	2.3612×10^{-15}
70	3.1950	3.1931	1.0031	1.3932	2.2204×10^{-16}	0	1.4803×10^{-16}	0	2.9266×10^{-15}	3.1576×10^{-15}
75	2.8348	2.6966	1.0677	0.8610	4.4409×10^{-16}	2.2204×10^{-16}	2.9606×10^{-16}	1.4803×10^{-16}	3.7614×10^{-15}	2.5670×10^{-15}
80	3.5043	2.3172	0.9581	0.8166	2.2204×10^{-16}	2.2204×10^{-16}	1.4803×10^{-16}	1.4803×10^{-16}	3.3670×10^{-15}	2.3426×10^{-15}
85	3.7103	2.7967	1.0677	0.7618	2.2204×10^{-16}	0	1.4803×10^{-16}	0	3.4057×10^{-15}	2.5169×10^{-15}

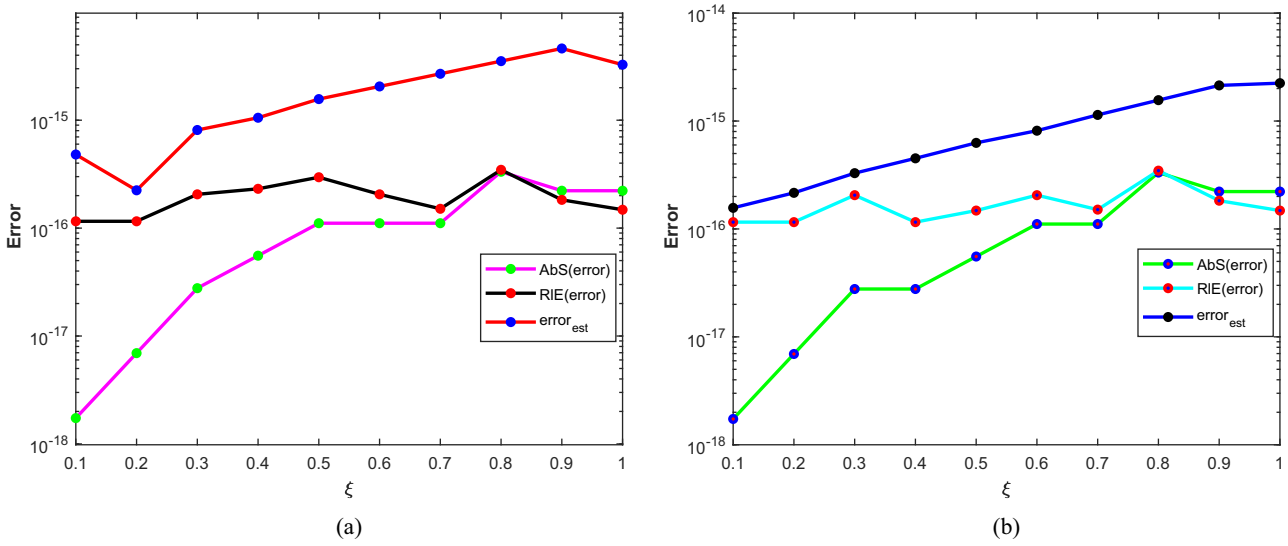

Figure 3: (a) The AbS(error), the RlE(error), and the $\text{error}_{\text{est}}$ *versus* ξ using $M = 65$ with ABD corresponding to problem 1. (b) The AbS(error), the RlE(error), and the $\text{error}_{\text{est}}$ *versus* ξ using $M = 65$ with CFD corresponding to problem 1.

4 Applications

This section illustrates the effectiveness of the Weeks method discussed earlier for the solution of BTE with CFD and ABD. Three numerical examples are used to support the proposed scheme. For all the numerical experiments, the fractional derivative $D_{\xi}^{\gamma+1}$ in (1) is considered in CFD and ABD sense with $0 < \gamma \leq 1$, and the fractional derivative D_{ξ}^{β} is considered in Caputo's sense with $\beta = 2$. The computational results demonstrate the accuracy and convergence of the proposed method. The absolute error (AbS(error)) and the relative error (RlE(error)) are used to measure the numerical error. The two error norms are defined as follows:

$$\text{AbS(error)} = |\mathcal{W}(\xi) - \mathcal{W}_{\text{Aprrox}}(\xi)|,$$

and

$$\text{RlE(error)} = \left| \frac{\mathcal{W}(\xi) - \mathcal{W}_{\text{Aprrox}}(\xi)}{\mathcal{W}(\xi)} \right|.$$

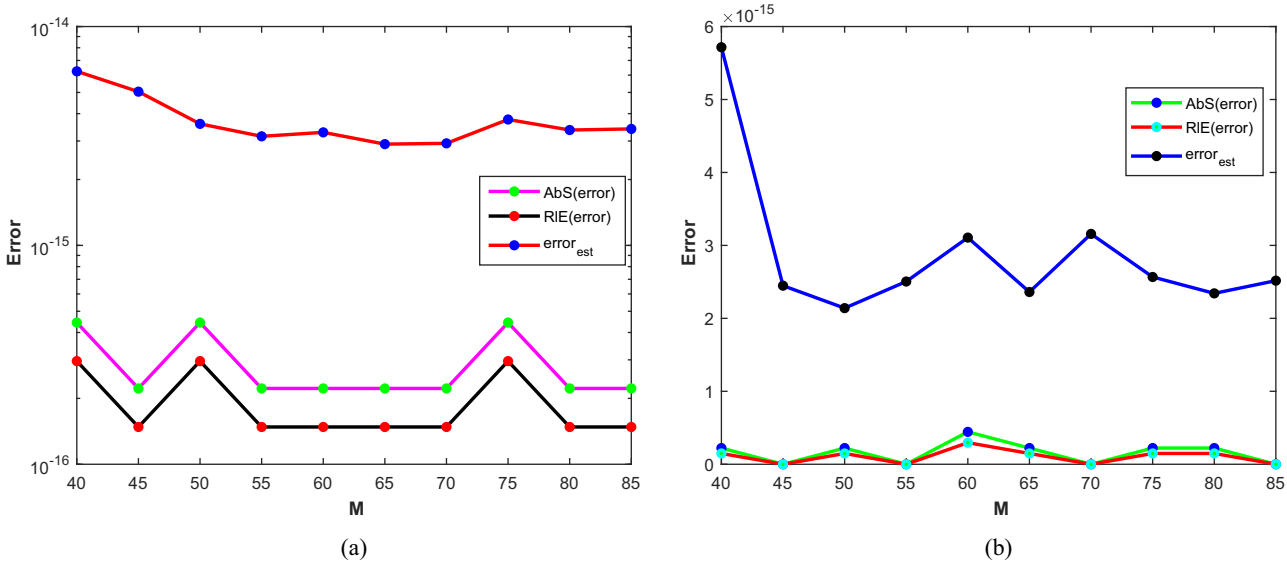

Figure 4: (a) The AbS(error), the RlE(error), and the $\text{error}_{\text{est}}$ *versus* M at $\xi = 1$ with ABD corresponding to problem 1. (b) The AbS(error), the RlE(error), and the $\text{error}_{\text{est}}$ *versus* M at $\xi = 1$ with CFD corresponding to problem 1.

Table 3: The AbS(error), RlE(error), and $\text{error}_{\text{est}}$ corresponding to Problem 2

ξ	σ		ς		AbS(error)		RlE(error)		$\text{error}_{\text{est}}$	
	ABD	CFD	ABD	CFD	ABD	CFD	ABD	CFD	ABD	CFD
0.1	3.3575	2.8414	1.0950	0.9623	8.8818×10^{-16}	8.8818×10^{-16}	2.0837×10^{-16}	2.0837×10^{-16}	3.3116×10^{-15}	3.6615×10^{-15}
0.2	3.2764	2.7190	1.4466	1.2817	8.8818×10^{-16}	8.8818×10^{-16}	1.9101×10^{-16}	1.9101×10^{-16}	4.6647×10^{-15}	4.7458×10^{-15}
0.3	3.1784	2.6885	1.0017	1.2230	8.8818×10^{-16}	8.8818×10^{-16}	1.7631×10^{-16}	1.7631×10^{-16}	6.1218×10^{-15}	6.0351×10^{-15}
0.4	3.2631	3.0666	1.0950	0.9623	1.7764×10^{-15}	2.6645×10^{-15}	3.2744×10^{-16}	4.9116×10^{-16}	8.3950×10^{-15}	8.0995×10^{-15}
0.5	3.2631	2.9472	1.0950	1.0843	8.8818×10^{-16}	2.6645×10^{-15}	1.5280×10^{-16}	4.5841×10^{-16}	1.1634×10^{-14}	1.0483×10^{-14}
0.6	3.2631	2.9472	1.0950	1.0843	1.7764×10^{-15}	2.6645×10^{-15}	2.8651×10^{-16}	4.2976×10^{-16}	1.6123×10^{-14}	1.4076×10^{-14}
0.7	3.3116	2.9472	1.5047	1.0843	8.8818×10^{-16}	1.7764×10^{-15}	1.3483×10^{-16}	2.6966×10^{-16}	2.4405×10^{-14}	1.8901×10^{-14}
0.8	3.3116	2.9472	1.5047	1.0843	2.6645×10^{-15}	3.5527×10^{-15}	3.8201×10^{-16}	5.0935×10^{-16}	3.3985×10^{-14}	2.5379×10^{-14}
0.9	3.2631	2.9472	1.0950	1.0843	1.7764×10^{-15}	5.3291×10^{-15}	2.4127×10^{-16}	7.2381×10^{-16}	4.2914×10^{-14}	3.4078×10^{-14}
1	3.2631	2.9472	1.0950	1.0843	2.6645×10^{-15}	6.2172×10^{-15}	3.4381×10^{-16}	8.0223×10^{-16}	5.9472×10^{-14}	4.5758×10^{-14}

The forcing term $f(\xi)$ and the initial boundary data are calculated using the exact solution for each example.

Problem 1

The first problem is solved using the Weeks method in ABD and CFD sense with exact solution $\mathcal{W}(\xi) = \gamma\xi^2$. In Table 1 the AbS(error), the RlE(error), and the $\text{error}_{\text{est}}$ for different values of ξ with $M = 65$ corresponding to Problem 1 are shown. Table 2 shows the AbS(error), the RlE(error), and the $\text{error}_{\text{est}}$ for different values of M at $\xi = 1$ corresponding to Problem 1. Figure 2 shows the plots of exact solution and Weeks solution. A comparison between the AbS(error), the RlE(error), and the $\text{error}_{\text{est}}$ of the proposed numerical scheme for problem 1 with ABD and CFD for different

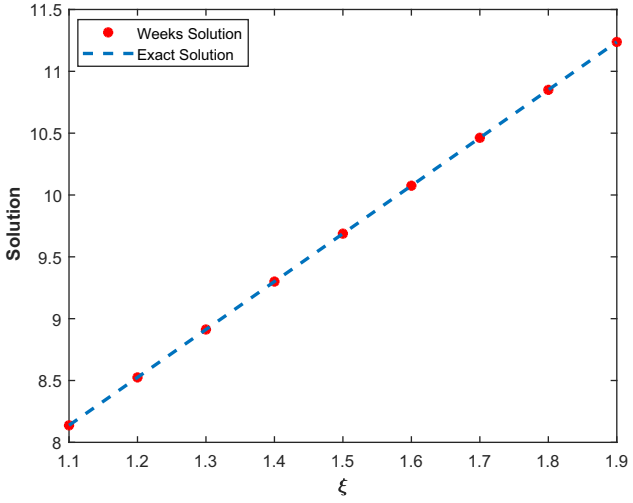

Figure 5: Exact solution *vs* Weeks solution of problem 2.

Table 4: The AbS(error), RlE(error), and $\text{error}_{\text{est}}$ corresponding to Problem 2

M	σ		ς		AbS(error)		RlE(error)		$\text{error}_{\text{est}}$	
	ABD	CFD	ABD	CFD	ABD	CFD	ABD	CFD	ABD	CFD
40	3.3361	2.1992	1.8698	1.4711	8.8818×10^{-16}	8.8818×10^{-16}	1.1460×10^{-16}	1.1460×10^{-16}	6.5568×10^{-14}	2.2671×10^{-14}
45	3.2776	2.2218	1.4159	0.9623	2.6645×10^{-15}	2.6645×10^{-15}	3.4381×10^{-16}	3.4381×10^{-16}	5.7867×10^{-14}	2.2004×10^{-14}
50	3.5237	2.2910	1.3375	1.2817	2.6645×10^{-15}	1.7764×10^{-15}	3.4381×10^{-16}	2.2921×10^{-16}	7.6392×10^{-14}	2.3616×10^{-14}
55	3.7631	2.7798	1.6532	1.5258	7.9936×10^{-15}	8.8818×10^{-16}	1.0314×10^{-15}	1.1460×10^{-16}	8.8526×10^{-14}	3.5755×10^{-14}
60	3.8559	2.7416	1.3935	1.1284	3.5527×10^{-15}	3.5527×10^{-15}	4.5841×10^{-16}	4.5841×10^{-16}	1.0943×10^{-13}	3.9962×10^{-14}
65	3.7631	2.8375	1.1383	0.8898	3.5527×10^{-15}	8.8818×10^{-16}	4.5841×10^{-16}	1.1460×10^{-16}	8.8963×10^{-14}	4.1297×10^{-14}
70	3.7116	2.8292	1.2984	0.7921	8.8818×10^{-16}	2.6645×10^{-15}	1.1460×10^{-16}	3.4381×10^{-16}	9.1073×10^{-14}	4.3553×10^{-14}
75	3.7854	2.8163	1.1004	0.9332	5.3291×10^{-15}	8.8818×10^{-16}	6.8762×10^{-16}	1.1460×10^{-16}	9.6980×10^{-14}	4.2486×10^{-14}
80	3.7244	2.7791	1.7039	0.7101	1.7764×10^{-15}	8.8818×10^{-16}	2.2921×10^{-16}	1.1460×10^{-16}	1.0826×10^{-13}	3.8936×10^{-14}
85	3.7146	2.6875	1.2202	0.7411	5.3291×10^{-15}	2.6645×10^{-15}	6.8762×10^{-16}	3.4381×10^{-16}	9.4354×10^{-14}	3.9239×10^{-14}

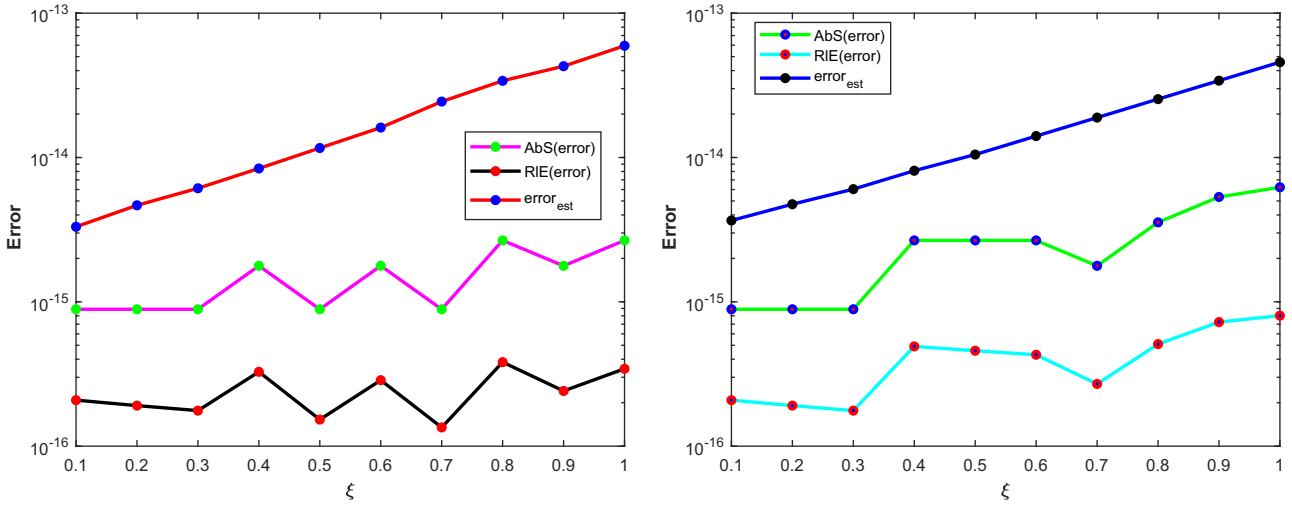

Figure 6: (a) The AbS(error), the RlE(error), and the $\text{error}_{\text{est}}$ *versus* ξ using $M = 65$ with ABD corresponding to problem 2. (b) The AbS(error), the RlE(error), and the $\text{error}_{\text{est}}$ *versus* ξ using $M = 65$ with CFD corresponding to problem 2.

values of ξ with $M = 65$ is shown in Figure 3(a) and (b), respectively. Similarly, the comparison between the AbS(error), the RlE(error), and the $\text{error}_{\text{est}}$ of the proposed numerical scheme for problem 1 with ABD and CFD for different values of M at $\xi = 1$ using the proposed method is shown in Figure 4(a) and (b), respectively. The results demonstrates the efficiency of the method for BTE with two different fractional derivatives.

Problem 2

The second problem is solved using the Weeks method with ABD and CFD and exact solution $\mathcal{W}(\xi) = (\gamma^3 + \gamma - 1)\xi + 1$. In Table 3, the AbS(error), the RlE(error), and the $\text{error}_{\text{est}}$ of the proposed method for different values of ξ with $M = 65$ corresponding to Problem 2 are presented. Table 4 shows the the AbS(error), the RlE(error), and the $\text{error}_{\text{est}}$ obtained

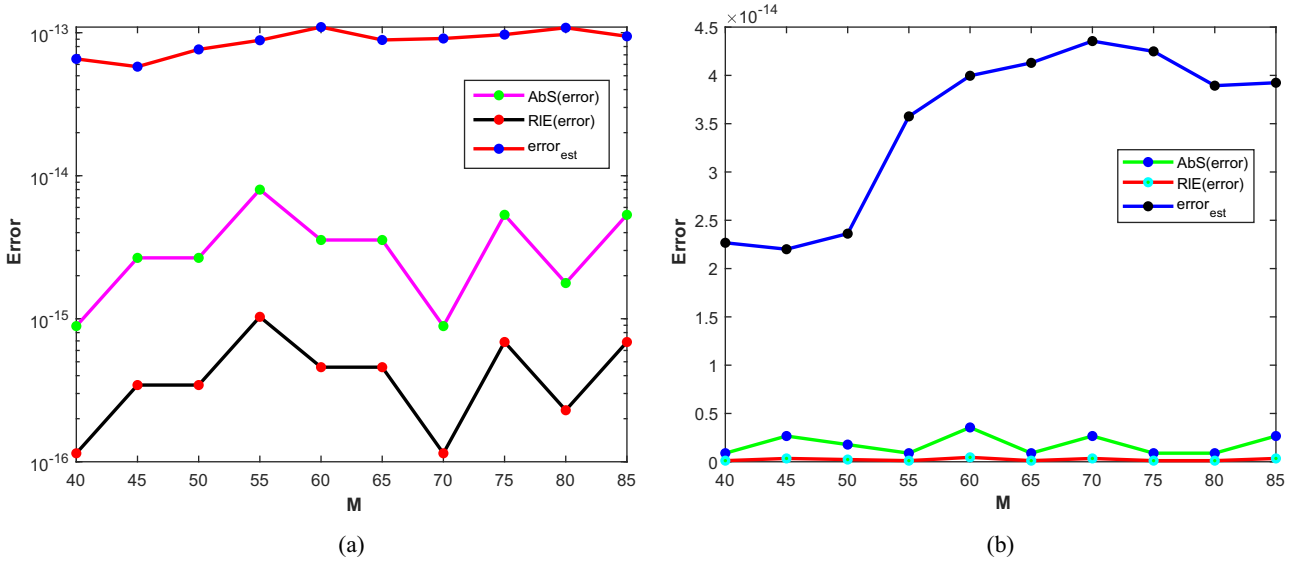

Figure 7: (a) The AbS(error), the RlE(error), and the $\text{error}_{\text{est}}$ *versus* M at $\xi = 1$ with ABD corresponding to problem 2. (b) The AbS(error), the RlE(error), and the $\text{error}_{\text{est}}$ *versus* M at $\xi = 1$ with CFD corresponding to problem 2.

Table 5: The AbS(error), RlE(error), and $\text{error}_{\text{est}}$ corresponding to Problem 3

ξ	σ		ς		AbS(error)		RlE(error)		$\text{error}_{\text{est}}$	
	ABD	CFD	ABD	CFD	ABD	CFD	ABD	CFD	ABD	CFD
0.1	3.4836	3.2814	1.1134	1.2312	2.7756×10^{-17}	5.5511×10^{-17}	1.2336×10^{-16}	2.4672×10^{-16}	3.5605×10^{-16}	4.1059×10^{-16}
0.2	3.5572	3.3504	1.2628	1.3932	5.5511×10^{-17}	1.1102×10^{-16}	1.2336×10^{-16}	2.4672×10^{-16}	5.5464×10^{-16}	5.9594×10^{-16}
0.3	2.8325	3.1001	0.9141	1.2111	2.2204×10^{-16}	1.1102×10^{-16}	3.2895×10^{-16}	1.6448×10^{-16}	8.6165×10^{-16}	8.2063×10^{-16}
0.4	2.8325	3.3397	0.9141	1.1870	1.1102×10^{-16}	2.2204×10^{-16}	1.2336×10^{-16}	2.4672×10^{-16}	1.1438×10^{-15}	1.0626×10^{-15}
0.5	2.8180	2.3605	0.9564	0.7803	2.2204×10^{-16}	2.2204×10^{-16}	1.9737×10^{-16}	1.9737×10^{-16}	1.6122×10^{-15}	1.2562×10^{-15}
0.6	2.4168	2.8056	0.9299	1.2600	4.4409×10^{-16}	2.2204×10^{-16}	3.2895×10^{-16}	1.6448×10^{-16}	1.9765×10^{-15}	1.9023×10^{-15}
0.7	2.8325	3.2416	0.9141	1.0171	2.2204×10^{-16}	2.2204×10^{-16}	1.4098×10^{-16}	1.4098×10^{-16}	2.6754×10^{-15}	2.8818×10^{-15}
0.8	2.8180	3.2416	0.9564	1.0171	4.4409×10^{-16}	2.2204×10^{-16}	2.4672×10^{-16}	1.2336×10^{-16}	3.7548×10^{-15}	3.9851×10^{-15}
0.9	2.8180	2.8348	0.9564	1.0144	4.4409×10^{-16}	4.4409×10^{-16}	2.1930×10^{-16}	2.1930×10^{-16}	4.9771×10^{-15}	4.5504×10^{-15}
1	2.4229	2.8348	0.7804	1.0144	4.4409×10^{-16}	4.4409×10^{-16}	1.9737×10^{-16}	1.9737×10^{-16}	4.7645×10^{-15}	6.0418×10^{-15}

using the proposed method for different values of M at $\xi = 1$ corresponding to Problem 2. Figure 5(a) shows the plots of exact solution and Weeks solution. A comparison between the AbS(error), the RlE(error), and the $\text{error}_{\text{est}}$ of the proposed numerical scheme for problem 1 with ABD and CFD for different values of ξ with $M = 65$ is shown in Figure 6(a) and (b), respectively. Similarly, the comparison between the AbS(error), the RlE(error), and the $\text{error}_{\text{est}}$ of the proposed method for problem 1 with ABD and CFD for different values of M at $\xi = 1$ using the proposed numerical scheme is shown in Figure 7(a) and (b), respectively. An excellent agreement between the theoretical and computed error is observed. In this case also, we see that the proposed numerical scheme has efficiently approximated the solution of BTE in both cases.

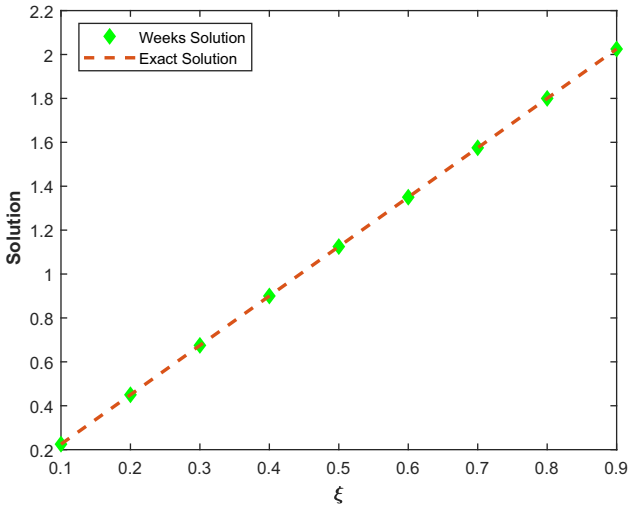

Figure 8: Exact solution *vs* Weeks solution of problem 3.

Table 6: The AbS(error), RlE(error), and $\text{error}_{\text{est}}$ corresponding to Problem 3

M	σ		ς		AbS(error)		RlE(error)		$\text{error}_{\text{est}}$	
	ABD	CFD	ABD	CFD	ABD	CFD	ABD	CFD	ABD	CFD
40	2.7218	2.4075	1.8961	1.1591	4.4409×10^{-16}	4.4409×10^{-16}	1.9737×10^{-16}	1.9737×10^{-16}	6.7274×10^{-15}	4.4139×10^{-15}
45	2.8798	2.7267	1.4047	1.3932	8.8818×10^{-16}	4.4409×10^{-16}	3.9475×10^{-16}	1.9737×10^{-16}	6.2411×10^{-15}	5.3304×10^{-15}
50	2.9416	2.6065	1.5047	1.0828	4.4409×10^{-16}	4.4409×10^{-16}	1.9737×10^{-16}	1.9737×10^{-16}	6.4160×10^{-15}	4.7877×10^{-15}
55	2.7754	3.0227	1.5047	1.1244	4.4409×10^{-16}	4.4409×10^{-16}	1.9737×10^{-16}	1.9737×10^{-16}	7.1677×10^{-15}	6.1922×10^{-15}
60	2.9242	3.4810	1.0137	1.3214	4.4409×10^{-16}	4.4409×10^{-16}	1.9737×10^{-16}	1.9737×10^{-16}	6.7855×10^{-15}	8.4881×10^{-15}
65	3.1167	3.0459	1.2628	1.3932	4.4409×10^{-16}	4.4409×10^{-16}	1.9737×10^{-16}	1.9737×10^{-16}	7.5523×10^{-15}	6.8758×10^{-15}
70	3.1341	3.1361	0.9299	1.0091	8.8818×10^{-16}	8.8818×10^{-16}	3.9475×10^{-16}	3.9475×10^{-16}	6.9303×10^{-15}	6.5436×10^{-15}
75	3.1167	2.8493	0.9299	0.8020	4.4409×10^{-16}	4.4409×10^{-16}	1.9737×10^{-16}	1.9737×10^{-16}	6.4809×10^{-15}	5.2802×10^{-15}
80	3.2249	3.2820	0.9299	0.8604	8.8818×10^{-16}	1.3323×10^{-15}	3.9475×10^{-16}	5.9212×10^{-16}	7.5662×10^{-15}	8.3731×10^{-15}
85	2.9590	3.1725	0.9299	0.8851	4.4409×10^{-16}	1.7764×10^{-15}	1.9737×10^{-16}	7.8949×10^{-16}	6.7840×10^{-15}	7.2423×10^{-15}

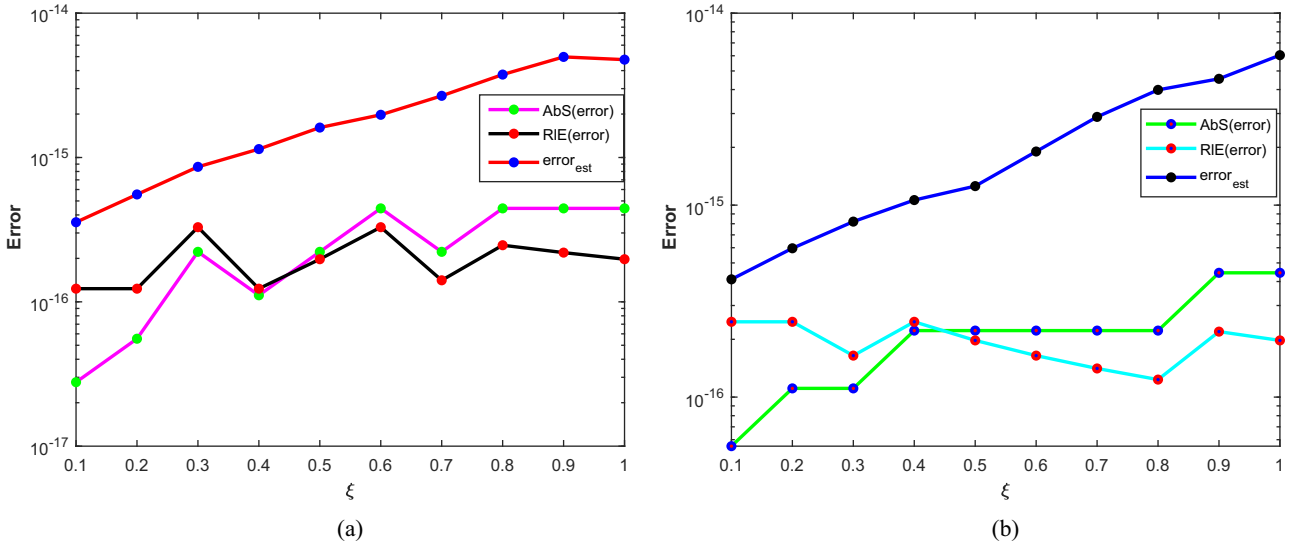

Figure 9: (a) The AbS(error), the RlE(error), and the $\text{error}_{\text{est}}$ *versus* ξ using $M = 65$ with ABD corresponding to problem 3. (b) The AbS(error), the RlE(error), and the $\text{error}_{\text{est}}$ *versus* ξ using $M = 65$ with CFD corresponding to problem 3.

Problem 3

The third problem is solved using the Weeks method with ABD and CFD and exact solution $\mathcal{W}(\xi) = \gamma^2\xi$. In Table 5, the AbS(error), the RlE(error), and the $\text{error}_{\text{est}}$ of the proposed method for different values of ξ with $M = 65$ corresponding to Problem 2 are presented. Table 6 shows the the AbS(error), the RlE(error), and the $\text{error}_{\text{est}}$ obtained using the proposed method for different values of M at $\xi = 1$ corresponding to Problem 2. Figure 8(a) shows the plots of exact solution and Weeks solution. A comparison between the AbS(error), the RlE(error), and the $\text{error}_{\text{est}}$ of the proposed numerical scheme for problem 1 with ABD and CFD for different values of ξ with $M = 65$ is shown in Figure 9(a) and (b), respectively. Similarly, the comparison between the AbS(error), the RlE(error), and the $\text{error}_{\text{est}}$ of the proposed numerical scheme for problem 1 with ABD and CFD for different values of M at $\xi = 1$ using the proposed numerical scheme is shown in Figure 10(a) and (b), respectively. We can see that for this problem also, the method has produced very accurate and stable results.

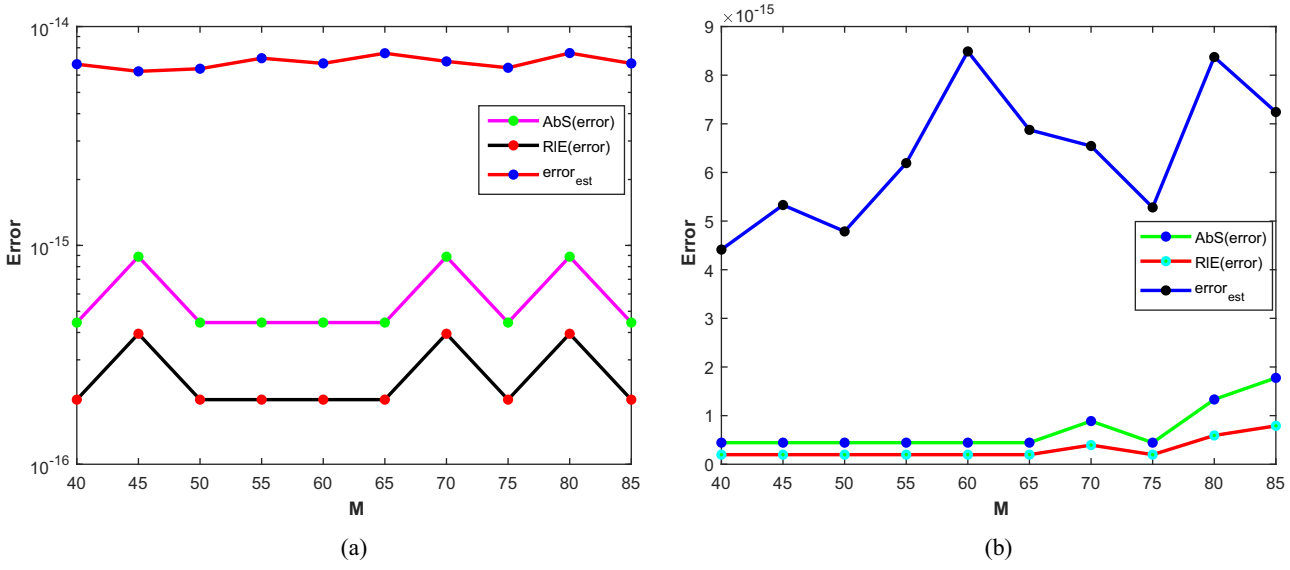

Figure 10: (a) The AbS(error), the RlE(error), and the $\text{error}_{\text{est}}$ *versus* M at $\xi = 1$ with ABD corresponding to problem 3. (b) The AbS(error), the RlE(error), and the $\text{error}_{\text{est}}$ *versus* M at $\xi = 1$ with CFD corresponding to problem 3.

5 Conclusion

The considered scheme has been applied for nonlocal and nonsingular fractional-order problems involving CFD and ABD. The proposed scheme has the ability to avoid discretization and complex calculation to approximate various problems of fractional orders. The computational cost is low as compared to other numerical or analytic methods for the considered problems. Our conclusion from this study is that: (i) This method provides a stable and accurate approach to the numerical calculation of the solutions to the considered BTEs, (ii) the method is highly sensitive to a proper choice for the two free parameters in the Laguerre expansion, and (iii) The proposed scheme is very easy to implement. In the future work, our aim is to use the proposed scheme coupled with some spatial discretization methods for numerical modeling of time-fractional PDEs.

Acknowledgments: Aiman Mukheimer, Kamal Shah, and Thabet Abdeljawad are thankful to Prince Sultan University for paying the APC and support through the TAS research lab.

Funding information: Aiman Mukheimer, Kamal Shah, and Thabet Abdeljawad are thankful to Prince Sultan University for paying the APC and support through the TAS research lab.

Author contributions: All authors have accepted responsibility for the entire content of this manuscript and approved its submission.

Conflict of interest: The authors state no conflict of interest.

References

[1] Diethelm K. The analysis of fractional differential equations. Berlin Heidelberg: Springer-Verlag; 2010.
[2] Podlubny I. Fractional differential equations. 1st ed. San Diego, CA, USA: Academic Press; 1999.
[3] Joseph D, Ramachandran R, Alzabut J, Jose SA, Khan H. A Fractional-order density-dependent mathematical model to find the better strain of Wolbachia. Symmetry. 2023;15(4):845.
[4] Joshi H, Yavuz M. Transition dynamics between a novel coinfection model of fractional-order for COVID-19 and tuberculosis via a treatment mechanism. Eur Phys J Plus. 2023;138(5):468.
[5] Torvik PJ, Bagley RL. On the appearance of the fractional derivative in the behavior of real materials. J Appl Mech. 1984;51(2):294–8
[6] Ji T, Hou J, Yang C. Numerical solution of the Bagley-Torvik equation using shifted Chebyshev operational matrix. Adv Differ Equ. 2020;2020(1):648.
[7] Ray SS, Bera RK. Analytical solution of the Bagley Torvik equation by Adomian decomposition method. Appl Math Comput. 2005;168(1):398–410.
[8] Jena RM, Chakraverty S. Analytical solution of Bagley-Torvik equations using Sumudu transformation method. SN Appl Sci. 2019;1:1–6.
[9] Çenesiz Y, Keskin Y, Kurnaz A. The solution of the Bagley-Torvik equation with the generalized Taylor collocation method. J Frank Inst. 2010;347(2):452–66.
[10] Mashayekhi S, Razzaghi M. Numerical solution of the fractional Bagley-Torvik equation by using hybrid functions approximation. Math Methods Appl Sci. 2016;39(3):353–65.
[11] Gülsu M, Öztürk Y, Anapali A. Numerical solution the fractional Bagley-Torvik equation arising in fluid mechanics. Int J Comput Math. 2017;94(1):173–84.
[12] Yüzbaşı Ş. Numerical solution of the Bagley-Torvik equation by the Bessel collocation method. Math Methods Appl Sci. 2013;36(3):300–12.
[13] Pinar Z. On the explicit solutions of fractional Bagley-Torvik equation arises in engineering. Int J Optim Control Theor Appl. 2019;9(3):52–8.
[14] Raja MAZ, Manzar MA, Shah SM, Chen Y. Integrated intelligence of fractional neural networks and sequential quadratic programming for Bagley-Torvik systems arising in fluid mechanics. J Comput Nonlinear Dyn. 2020;15(5):051003.
[15] Kilbas AA, Srivastava HM, Trujillo JJ. Theory and applications of fractional differential equations. Vol. 204. Amsterdam: Elsevier; 2006.
[16] Caputo M, Fabrizio M. A new definition of fractional derivative without singular kernel. Prog Fract Differ Appl. 2015;1(2):73–85.
[17] Atangana A, Alqahtani RT. Numerical approximation of the space-time Caputo–Fabrizio fractional derivative and application to groundwater pollution equation. Adv Differ Equ. 2016;2016(1):1–13.
[18] Hasan S, Djeddi N, Al-Smadi M, Al-Omari S, Momani S, Fulga A. Numerical solvability of generalized Bagley-Torvik fractional models under Caputo–Fabrizio derivative. Adv Differ Equ. 2021;2021(1):1–21.
[19] Al-Smadi M, Djeddi N, Momani S, Al-Omari, S, Araci S. An attractive numerical algorithm for solving nonlinear Caputo–Fabrizio fractional Abel differential equation in a Hilbert space. Adv Differ Equ. 2021;2021(1):1–18.
[20] Moore EJ, Sirisubtawee S, Koonprasert S. A Caputo–Fabrizio fractional differential equation model for HIV/AIDS with treatment compartment. Adv Differ Equ. 2019;2019(1):1–20.
[21] Joshi H, Yavuz M, Stamova I. Analysis of the disturbance effect in intracellular calcium dynamic on fibroblast cells with an exponential kernel law. Bull Bio Math. 2023;1(1):24–39.
[22] Kamal R, Kamran, Rahmat G, Ahmadian A, Arshad NI, Salahshour S. Approximation of linear one dimensional partial differential equations including fractional derivative with non-singular kernel. Adv Differ Equ. 2021;2021(1):1–15.
[23] Kamran A A, Gómez-Aguilar JF. A transform based local RBF method for 2D linear PDE with Caputo–Fabrizio derivative. Comptes Rendus Math. 2020;358(7):831–42.
[24] Ahmed I, Akgül A, Jarad F, Kumam P, Nonlaopon K. A Caputo–Fabrizio fractional-order Cholera model and its sensitivity analysis. Math Model Numer Simul Appl. 2023;3(2):170–87.
[25] Atangana A, Baleanu D. New fractional derivatives with nonlocal and non-singular kernel: theory and application to heat transfer model. Therm Sci. 2016;20:763–9.

[26] Atangana A, Koca I. Chaos in a simple nonlinear system with Atangana–Baleanu derivatives with fractional order. Chaos Solitons Fractals. 2016;89:447–54.
[27] Kamran, Ahmadian A, Salahshour S, Salimi M. A robust numerical approximation of advection diffusion equations with nonsingular kernel derivative. Phys Scr. 2021;96(12):124015.
[28] Atangana A. On the new fractional derivative and application to nonlinear Fisher's reaction-diffusion equation. Appl Math Comput. 2016;273:948–56.
[29] Gómez-Aguilar JF, Escobar-Jiménez RF, López-López MG, Alvarado-Martínez VM. Atangana–Baleanu fractional derivative applied to electromagnetic waves in dielectric media. J Electromagn Waves Appl J. 2016;30(15):1937–52.
[30] Ghanbari B, Günerhan H, Srivastava HM. An application of the Atangana–Baleanu fractional derivative in mathematical biology: A three-species predator-prey model. Chaos Solitons Fractals. 2020;138:109910.
[31] Khan H, Alzabut J, Gulzar H. Existence of solutions for hybrid modified ABC-fractional differential equations with p-Laplacian operator and an application to a waterborne disease model. Alex Eng J. 2023;70:665–72.
[32] Joshi H, Yavuz M, Townley S, Jha BK. Stability analysis of a non-singular fractional-order covid-19 model with nonlinear incidence and treatment rate. Phys Scr. 2023;98(4):045216.
[33] Kamran AM, Shah K, Abdalla B, Abdeljawad T. Numerical solution of Bagley-Torvik equation including Atangana–Baleanu derivative arising in fluid mechanics. Results Phys. 2023;49:106468.
[34] Khan H, Alzabut J, Alfwzan WF, Gulzar H. Nonlinear dynamics of a piecewise modified ABC fractional-order leukemia model with symmetric numerical simulations. Symmetry. 2023;15(7):1338
[35] Yavuz M, Özdemir N. Comparing the new fractional derivative operators involving exponential and Mittag–Leffler kernel. Discrete Cont Dyn-S. 2020;13(3):1–12.
[36] Atangana A, Araz Sİ. Step forward on nonlinear differential equations with the Atangana–Baleanu derivative: Inequalities, existence, uniqueness and method. Chaos Solitons Fractals. 2023;173:113700.
[37] Qureshi S, Yusuf A. Modeling chickenpox disease with fractional derivatives: from Caputo to Atangana–Baleanu. Chaos Solitons Fractals. 2019;122:111–8.
[38] Arık İA, Araz Sİ. Crossover behaviors via piecewise concept: a model of tumor growth and its response to radiotherapy. Results Phys. 2022;41:105894.
[39] Davies B, Martin B. Numerical inversion of the Laplace transform: a survey and comparison of methods. J Comput Phys. 1979;33(1):1–32.
[40] Duffy DG. On the numerical inversion of Laplace transforms: comparison of three new methods on characteristic problems from applications. ACM Trans Math Softw. 1993;19(3):333–59.
[41] Abate J, Choudhury GL, Whitt W. On the Laguerre method for numerically inverting Laplace transforms. Informs J Comput. 1996;8(4):413–27.
[42] Brio M, Kano PO, Moloney JV. Application of Weeks method for the numerical inversion of the Laplace transform to the matrix exponential. Commun Math Sci. 2005;3(3):335–72.
[43] Weideman JAC. Algorithms for parameter selection in the Weeks method for inverting the Laplace transform. SIAM J Sci Comput. 1999;21(1):111–28.